JOURNAL OF SOLID STATE CHEMISTRY 107, 480–488 (1993)

Structure, Bonding, and Properties of $CaZn_{1-x}Cd_xSn$ and $CaSn_{0.5}Ge_{1.5}$*

A. K. GANGULI AND J. D. CORBETT

Ames Laboratory–DOE† and Department of Chemistry, Iowa State University, Ames, Iowa 50011

Received February 18, 1993; accepted April 13, 1993

CaZnSn, the end member of the $CaZn_{1-x}Cd_xSn$ series, crystallizes in the LiGaGe structure type, an ordered ternary version of $CaIn_2$ (space group $P6_3mc$, $Z = 2$, $a = 4.621(2)$ Å, $c = 7.643(2)$ Å). Alternating Zn and Sn form puckered hexagonal layers that are interconnected by 0.40 Å longer Zn–Sn bonds (around intercalated Ca) to form a distorted wurtzite-like framework. This structure is retained through $x = 0.75$. The other member, CaCdSn, has the Fe_2P structure type (space group $P\bar{6}2m$, $Z = 4$, $a = 7.6319(5)$, $c = 4.6996(4)$ Å) and consists of two kinds of augmented trigonal prisms of Ca and Cd centered by different Sn atoms. $CaSn_{0.52(2)}Ge_{1.48(2)}$ crystallizes in the $P6_3mc$ space group ($a = 4.117(1)$, $c = 10.300(3)$ Å) and has the KSnAs structure, with puckered ordered layers of Sn and Ge separated by calcium. The composition is the tin-rich limit of stability. The $CaZn_{1-x}Cd_xSn$ phases for $x = 0$, 0.25, 0.50 are weak Pauli paramagnets and poor metals (~50 $\mu\Omega \cdot$ cm at 290 K). Distortions of the hexagonal wurtzite-based matrix by the inserted Ca are thought to be responsible for this unexpected result. CaCdSn and $CaSn_{0.5}Ge_{1.5}$ are diamagnetic although the former shows a nearly temperature-independent resistivity of ~35 $\mu\Omega \cdot$ cm. © 1993 Academic Press, Inc.

Introduction

Certain Ca–Pb–Z systems have been found to form particularly novel Ca_5Pb_3Z phases (Z = V–Ni, Zn, Cd) with stuffed Mn_5Si_3-type ($P6_3/mcm$) structures (*1*). We sought to develop the same aspects of the presumably closely related Ca–Sn–Z systems but obtained only other phases. However, early transition metals as Z yielded substituted tetragonal W_5Si_3-type structures (*2*), as they do for Zr_5Sb_3Z and Zr_5Sn_3Z (*3*), while the late members of the above series produce the hexagonal ABX phases CaZnSn and CaCdSn. These two have been reported earlier from powder data (*4*), but their different structures and properties have evidently not been investigated. The 1 : 1 : 1 composition CaSnGe was also investigated and found to produce the unexpected Ca $Sn_{0.5}Ge_{1.5}$. The present article reports on these syntheses, including within the $CaZn_{1-x}Cd_xSn$ system, the crystal structures of the three phases noted above, and some magnetic and electronic conductivity properties.

Experimental

Syntheses

The compounds were synthesized from high purity elements. Dendritic Ca (99.99%,

* The submitted manuscript has been authored by a contractor of the U.S. Government under contract No. W-7405-ENG-82. Accordingly, the U.S. Government retains a nonexclusive, royalty-free license to publish or reproduce the published form of this contribution, or allow others to do so for U.S. Government purposes.

† The Ames Laboratory is operated for DOE by Iowa State University under contract No. W-7405-Eng-82. This research was supported by the Office of the Basic Energy Sciences, Materials Sciences Division, U.S. Department of Energy.

0022-4596/93 $5.00

Copyright © 1993 by Academic Press, Inc.
All rights of reproduction in any form reserved.

APL Eng. Mat.), Sn bar (99.99%, Baker's Analyzed), Zn granules (99.999%, J. T. Baker), Ge pieces (99.99% Aesar) and Cd strips (Comico) were used for the syntheses. The calcium and all the products were stored and handled only in a helium or nitrogen-filled glovebox. Stoichiometric amounts of the elements were loaded in Ta tubes which were then welded under a helium atmosphere. These were in turn jacketed within evacuated, fused silica containers and heated in resistance furnaces at 1100°C or below. The reaction periods varied from 5 to 15 days. Reaction conditions that gave homogeneous phases were 875°C for 1 day, cooling to 750°C at 5°C/hr, and annealing there for 3 days. The Ca $Zn_{1-x}Cd_xSn$ phases were aluminum-like in appearance with a dull hue for $x \leq 0.75$, while CaCdSn and $CaSn_{0.5}Ge_{1.5}$ had a dull reflectance and a yellow or golden tinge.

Powder X-Ray Diffraction

Powder patterns were obtained on samples mounted between pieces of cellophane tape. An Enraf-Nonius Guinier camera, Cu$K\alpha_1$ radiation, and NBS (NIST) silicon as an internal standard were employed for this purpose. The known 2θ values of the standard lines were fitted to a quadratic in their positions on the film, and lattice constants of the samples then calculated by least-squares fit of indexed lines with 2θ values deduced with the aid of the calibration lines.

Properties

Magnetic susceptibility samples were held in between two silica rods fixed within a silica tube. The assembly was evacuated, back-filled with helium, and sealed. The susceptibilities were measured at 3T or 5T over the range 6–298 K on a Quantum Design SQUID magnetometer. The raw data were corrected for both the susceptibility of the container and the diamagnetic susceptibility of the ion cores. All data were "temperature independent" within ±(1–10)% between 298 and 15 to 60 K. Electrical conductivity data were obtained as a function of temperature between 150 and ~290 K by an electrodeless "Q" method at ~35 MHz (*5*). Powdered samples averaging 500 μm in diameter were mixed with equal volumes of chromatographic Al_2O_3. The ρ values are thought to be accurate within a factor of three, and this is in accord with our experiences.

Single-Crystal Structure Determinations

Crystals were picked from crushed samples and mounted in glass capillaries within the glovebox. Oscillation photographs were used to check the quality of the crystals. Single crystal diffraction data were collected at room temperature with the aid of Rigaku AFC6R or CAD-4 four-circle diffractometers together with monochromated MoKα radiation. Details of the data collections and refinements are listed in Table I. The ~25 reflections found from a random search by the diffractometer were indexed and the Laue symmetry deduced from supposedly symmetry-equivalent reflections. Only the statistics for the CaZnSn data were clear about a probable acentricity. The diffraction data were corrected for Lorentz and polarization effects and for absorption using the average of ψ scans of three reflections at different θ values. A final absorption correction with DIFABS (*6*) was applied to the data for structure three before anisotropic refinement. Direct methods (SHELXS (*7*)) were used in each case to obtain an initial model. Least-squares refinement using the TEXSAN package (*8*) led to smooth convergence of all positional and anisotropic thermal parameters. Refinement of the other enantiomer was performed in all three cases to establish the assignment. The refined coordinates have been transformed when necessary to match the selection reported for the parent compounds. The F_o/F_c listings are available from J.D.C.

Results and Discussion

$CaZn_{1-x}Cd_xSn$ ($0.0 \leq x \leq 0.75$)

Monophasic samples of CaZnSn and of solid solutions with $x = 0.25, 0.50, 0.75$ were synthesized as described in the Experimental section. Their powder patterns could be completely indexed with a hexagonal cell and lattice parameters that increased with x, Table II. There is also a systematic decrease in c/a in the same direction.

A single crystal study of CaZnSn was carried out in order to investigate the structural details. The indicated Laue group $P6/mmm$ and the systematic absences for hhl, $l = 2n$, suggested space groups $P6_3mc$, $P\bar{6}2c$, or $P6_3/mmc$. The structure was satisfactorily solved and refined in the first. Some information on the collection and refinement processes is listed in Table I, and positional and anisotropic thermal parameters and interatomic distances are given in Table III. As deduced from powder data by Iandelli (*4*), CaZnSn is isostructural with the Li GaGe (or LiZnSb) prototype with the respective atom positions. The structure is built from puckered 6^3 graphite-like layers in which Zn and Sn occupy alternate positions in each six-membered ring, Fig. 1a. There is negligible mixing between the two sites. The Ca atoms lie over the centers of the puckered hexagons. From another point of view (Fig. 1b), the Ca atoms themselves form trigonal prisms which share faces in all three directions, and the Zn and Sn atoms are alternatively shifted up or down along **c** from the prism centers. This gives a 0.48 Å asymmetry to Ca–Zn distances and 0.26 Å differences in Ca–Sn distances. The drive for more or less tetrahedral bonding within the layers is presumably responsible.

The present structure type derives directly from that of $CaIn_2$ ($P6_3/mmc$ (*9*) on reduction of symmetry to allow for alternat-

TABLE I

SUMMARY OF DATA COLLECTION AND REFINEMENT PARAMETERS

	CaZnSn	CaCdSn	$CaSn_{0.52(2)}Ge_{1.48(2)}$
Crystal size, mm	0.1 × 0.08 × 0.04	irregular	irregular
Lattice parameters, Å	[a]	[a]	4.117(1), 10.300(3)
V, Å^3	143.1(1)	237.06(5)	151.19(7)
Space group, Z	$P6_3mc$, (No. 186), 2	$P\bar{6}2m$ (No. 189), 2	$P6_3mc$ (No. 186), 2
Diffractometer	Rigaku AFC6R	CAD-4	CAD-4
Temperature, °C	23	23	23
Octants measured	$h, k, \pm l$	$-h, k, \pm l$	$h, \pm k, \pm l$
Scan mode	$\omega - 2\theta$	$\omega - 2\theta$	$\omega - 2\theta$
$2\theta_{max}$	50	50	50
Total refl. meas.	240	627	600
Unique reflections	144	182	160
Indep. obs. refln. ($I \geq 3\sigma(I)$)	98	167	122
μ (Mo $K\alpha$) cm^{-1}	187.63	159.26	201.68
Transm. coeff. range	0.859–1.00	0.649–1.00	0.839–1.101
Variables	10	14	11
R_{ave} (all data)	0.041	0.045	0.076
Residuals R; R_w[b]	0.025; 0.029	0.023; 0.027	0.025; 0.028
Goodness of fit	1.221	1.189	1.444
$(\Delta\rho)_{max}$, $(\Delta\rho)_{min}$, e/Å^3	1.2, −1.8	0.72, −1.8	0.83, −1.9
Secondary ext. coeff.	3.7(8) × 10^{-6}	5.5(4) × 10^{-6}	—

[a] See Table II.

[b] $R = \Sigma||F_o| - |F_c||/\Sigma|F_o|$; $R_w = [\Sigma w(|F_o| - |F_c|)^2/\Sigma w(F_o)^2]^{1/2}$; $w = \sigma_F^{-2}$.

TABLE II

THE $CaZn_{1-x}Cd_xSn$ SYSTEM: CRYSTAL DATA AND SOME PHYSICAL PROPERTIES

x	Space group	a (Å)[a]	c (Å)[a]	c/a	χ_M[b] (10^{-4} emu/mole)	ρ_{290} $\mu\Omega \cdot$ cm	$d\rho/dT$ $\mu\Omega \cdot$ cm K^{-1}
0.00	$P6_3mc$	4.655(1)	7.628(3)	1.639	2.54	67	0.38
0.25	$P6_3mc$	4.702(2)	7.661(5)	1.629	2.19	—	—
0.50	$P6_3mc$	4.7452(2)	7.6833(8)	1.619	0.30	35	0.24
0.75	$P6_3mc$	4.7964(3)	7.723(1)	1.610	−0.54[c]	45	0.10
1.00	$P\bar{6}2m$	7.6319(5)	4.6996(4)	0.6158	−0.65[c]	34	0.04

[a] From Guinier powder data, $\lambda = 1.54056$ Å.
[b] Corrected for core diamagnetism.
[c] Measured at 5 T.

ing main-group elements in the puckered layers. It can also be viewed as an isoelectronic $ZnSn^{2-}$ version of ZnTe (wurtzite) with Ca^{2+} ions in octahedral sites. The wurtzite-like framework is substantially distorted, the interlayer Zn–Sn bonds (3.168 Å, lighter lines in Fig. 1a) being substantially longer than within the hexagons (2.764 Å). Accommodation of the relatively large calcium appears to be responsible for this distortion as well as, perhaps, a flattening of the layers. Rather short Ca–Zn distances in

TABLE III

POSITIONAL AND THERMAL PARAMETERS[a] AND REFINED DISTANCES (Å) AND ANGLES (deg) FOR CaZnSn ($P6_3mc$)

Atom	x	y	z	B_{equ}[b]
Ca	0	0	0.2470(8)	1.2(1)
Zn	$\frac{1}{3}$	$\frac{2}{3}$	0.0518(5)	1.6(1)
Sn	$\frac{1}{3}$	$\frac{2}{3}$	0.4670	0.95(5)

	U_{11}	U_{22}	U_{33}
Ca	0.016(2)	U_{11}	0.015(4)
Zn	0.014(1)	U_{11}	0.033(2)
Sn	0.0106(8)	U_{11}	0.015(1)

Ca–Ca (×2)	3.814(2)	Zn–Ca (×3)	3.073(4)
Ca–Sn (×3)	3.169(4)	Zn–Ca (×3)	3.554(6)
Ca–Sn (×3)	3.433(4)	Zn–Sn (×3)	2.764(1)
Ca–Zn (×3)	3.073(4)	Zn–Sn (×1)	3.168(4)
Ca–Zn (×3)	3.554(6)		
Sn–Zn (×3)	2.764(1)	Sn–Zn–Sn (×3)	103.53(8)
Sn–Zn (×1)	3.168(4)	Sn–Zn–Sn (×3)	114.70(6)
Sn–Ca (×3)	3.169(4)	Ca–Sn–Zn (×3)	58.02(9)
Sn–Ca (×3)	3.433(4)	Ca–Sn–Zn (×3)	128.47(9)

[a] $T = \exp[-2\pi^2(U_{11}h^2a^{*2} + U_{22}k^2b^{*2} + U_{33}l^2c^{*2} + 2U_{12}hka^*b^* + 2U_{13}hla^*c^* + 2U_{23}klb^*c^*)]$; $U_{12} = U_{11}/2$, $U_{13} = U_{23} = 0$.
[b] Refined occupancies of 0.95(2) for Zn, 1.00(2) for Sn were reset to unity in final cycles.

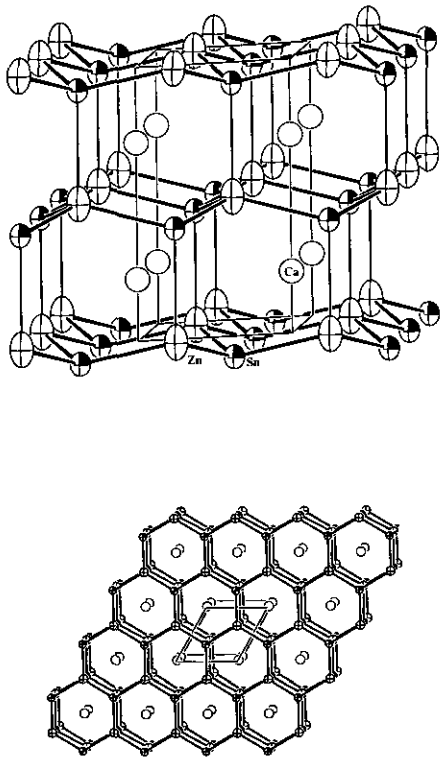

FIG. 1. (a) A side view of the layers in the CaZnSn (LiGaGe-type) structure with Ca, Zn, and Sn as open, crossed, and shaded ellipsoids, respectively (94% probability). The lighter vertical lines between Zn and Sn mark the 0.40 Å longer interlayer bonds. (b) A projection slightly off [001] of CaZnSn with the cell outlined.

particular, 0.10 to 0.20 Å less than in $CaZn_3$ (*10*) and Ca_3Zn (*11*), are additional evidence of such strain, while the Ca–Sn separations, which probably involve the more negative member, are near the middle of the range found in $Ca_{31}Sn_{20}$ (*2*). It is noteworthy that this framework persists on substitution of more than 75% of the Zn by the larger Cd, presumably with some relief of the strain, but it converts to different arrangement for CaCdSn (below). This structure also exists with YbZnSn but not with larger cations unless in a larger framework (EuCdSn, EuCdPb) (*12*).

The dozen or so members known in the ternary LiCaGe structure type (*13*) all contain eight valence electrons. Most are composed of only main-group elements as in CaZnSn, but this electronic classification also reasonably applies to a few compounds of late transition metal compounds if Pt is closed shell (d^{10}) in NdPtSb and Au(I) pertains in CaAuSb. (The inclusion of one study of the structure of KSnAs in this category (*13*) rather than in its own 10-electron family (below) was not implied by the original report (*14*) and must be a classification error or a misprint.)

A much larger number of compounds of this charge type are known in a variety of other structure types (zinc blende, Ni_2In, $CaIn_2$, Cu_2Sb, $CaSi_2$, etc. and ternary versions). In some members, an element from the Ni or Cu family replaces one of the post-transition elements. These have been extensively investigated by Schuster (*15*), who notes that these are all semiconductors as far as is known. LiMgAuSn, ScAuSn, MgAuSb (zinc-blende), NaZnAs, and Li InGe) (CaF_2-type) are specifically so described. The wurtzite-based CaZnSn and related phases would ordinarily be expected to be diamagnetic semiconductors as well. Surprisingly, the $CaZn_{1-x}Cd_xSn$ phases show a weak Pauli-like paramagnetism for $x \leq 0.5$, with a magnitude that decreases with an increase in Cd concentration so that the phases for $x = 0.75$, 1.00 are diamagnetic (Table II). Subsequent resistivity measurements on powders by the "Q" method (*5*) are supportive. As also shown in Table II, CaZnSn and $CaZn_{0.5}Cd_{0.5}Sn$ exhibit metal-like resistivities and, in particular, positive temperature coefficients of 0.38 and 0.24 $\mu\Omega \cdot cm\ K^{-1}$, respectively. The $CaZn_{0.25}Cd_{0.75}Sn$ and CaCdSn samples gave comparable resistivities but with distinctly smaller coefficients, 0.10 and 0.04 $\mu\Omega \cdot cm\ K^{-1}$, in parallel with their clear diamagnetism. A plausible explanation of the more pronounced anomalies with the zinc-richer members could derive from the substantial elongation of one of the four "tetrahedral" Zn–Sn bonds that accompanies the formation of well defined layers (above). This 0.4 Å difference is equivalent to a bond order reduction of ~75–80%. Such a distortion

could cause corresponding portions of the conventional valence and conduction bands in $ZnSn^{2-}$ to split off and converge, evidently overlapping to give the observed metallic behavior. The band overlap, or unidentified intrinsic effects, presumably diminish with substitution of the larger Cd (note that c/a decreases at the same time). Physical measurements on most presumed Zintl phases have not been reported, and we are not aware of any theoretical studies of the particular aspect encountered here either.

CaCdSn

The end member of the CaCdSn series crystallizes in a different, Fe_2P-type structure. Lattice parameters of this phase reported before (*4*) agree with those determined here (Table I) within the larger errors given in the former. The single crystal study was undertaken to understand the detailed structure and to confirm that the Ca and Cd positions are fully ordered, as they are. The indicated Laue group $P6/mmm$ and the absence of systematic extinctions in the diffraction data suggested space group $P\bar{6}2m$, $P6mm$ or $P6/mmm$, and the structure was successfully refined in the first. The positional and thermal parameters and some distances are given in Table IV. The higher coordination number possible for Cd (9) vs Zn (6) probably drives this structure choice within the $CaZn_{1-x}Cd_xSn$ system. Trigonal prisms of Cd and Ca are centered by Sn1 and Sn2, respectively, with the latter prisms sharing side edges, Fig. 2. These two types of trigonal prisms are stacked with displacements of $c/2$ so that three Ca and Cd atoms face-cap the prisms with and are also neighbors to Sn1 and Sn2, respectively. The structure is properly described as a ternary member of the Fe_2P family since this lattice is crystallographically quarternary with

TABLE IV

POSITIONAL AND THERMAL PARAMETERS AND DISTANCES (Å) IN CaCdSn ($P\bar{6}2m$)

	x	y	z	B_{eq}	Occup.[a]
Ca (3*g*)	0.5736(6)	0	½	1.1(2)	0.96(1)
Cd (3*f*)	0.2509(1)	0	0	1.23(6)	1
Sn1 (1*b*)	0	0	½	0.99(5)	1.01(1)
Sn2 (2*c*)	⅓	⅔	0	0.81(7)	1.004(6)
	U_{11}	U_{22}	U_{33}[b]		
Ca	0.015(1)	0.013(2)	0.014(2)		
Cd	0.0144(6)	0.0157(7)	0.0169(7)		
Sn1	0.0134(6)	U_{11}	0.011(1)		
Sn2	0.0107(5)	U_{11}	0.0091(7)		
Ca–Sn1	3.253(4)		Sn1–Cd (×6)	3.031(7)	
Ca–Sn2 (×4)	3.2700(7)		Sn1–Ca (×3)	3.253(4)	
Ca–Cd (×2)	3.405(3)				
Ca–Cd (×4)	3.680(3)		Sn2–Ca (×6)	3.2700(7)	
Ca–Ca (×4)	3.939(2)		Sn2–Cd (×3)	2.9101(8)	
Cd–Sn1 (×2)	3.0311(7)				
Cd–Sn2 (×2)	2.9101(8)				
Cd–Cd (×2)	3.316(2)				
Cd–Ca	3.405(3)				
Cd–Ca	3.680(3)				

[a] Reset to unity in final cycles.
[b] $U_{12} = U_{22}/2$; $U_{13} = U_{23} = 0$.

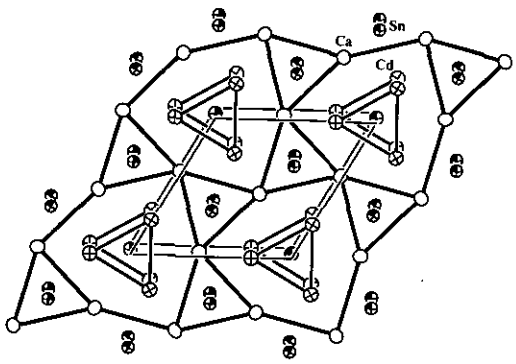

FIG. 2. ~[001] projection of the structure of CaCdSn (Fe_2P-type) with Ca, Cd, and Sn as open, crossed, and shaded (94%) ellipsoids, respectively. Note that the Ca and Cd trigonal prisms about Sn2 and Sn1, respectively, are displaced by $c/2$ so that the former atoms also cap rectangular faces of the other prism type. (The c axes pass through Sn1.)

pairs of independent cation and anion sites in proportions 3 : 3 : 1 : 2 (*16*). (The ZrNiAl identification sometimes used may not be suitable since this phase may exhibit a superstructure (*13*).) The ordering of Ca vs Cd in cation sites as well as Cd vs Sn in this structure likely arise from the distinctly smaller effective radius of the second element in each pair as well as the greater polarity (and number) of Ca–Sn interactions. Although Cd and Sn are not well distinguished by their scattering powers for X-rays, exchange of their positions in the structure causes Cd in the assigned Sn sites to refine with a clear excess occupancy (13(2)%). CaCdGe, CaCdPb, and YbCdSn have the same structure according to powder data (*4*, *12*).

The diamagnetism of CaCdSn (Table II) indicates a relatively small number of free carriers, although a semiconducting characteristic for this phase is not as clear (Table II). A Zintl phase classification (*17*) in terms of oxidation states would be Ca^{2+}, Cd^{2+} and (isolated) Sn^{4-}, but some covalency is to be expected and would not alter this picture. Although this description is probably useful to describe the more tightly bound valence electrons, it is clear from the conductivity that appreciable electronic mobility must be present at or near E_F.

$CaSn_{0.5}Ge_{1.5}$

The 10-electron composition CaGeSn was also investigated in part because $CaSn_2$ is unknown although $CaSi_2$ and $CaGe_2$ both occur in the former structure type. Instead, a composition $CaSn_{0.5}Ge_{1.5}$ was established by a structural study (see Fig. 3). Orientation studies of the plate-like crystals on the diffractometer suggested the Laue-group $P6/mmm$, and systematic absences $\ell = 2n$ for $hh\ell$ supported space groups $P6_3mc$, $P\bar{6}2c$, or $P6_3/mmc$. The statistics of the intensity distribution were not very clear about centricity, but the structure was refined satisfactorily in the first, acentric member. The results, Table V, correspond to a refined composition $CaSn_{0.52(2)}Ge_{1.48(2)}$. The second metalloid position has substantially equal amounts of Ge and Sn when these are constrained to have the same positional and anisotropic thermal parameters, and the site is assumed to be fully occupied. This composition pertains to the phase in

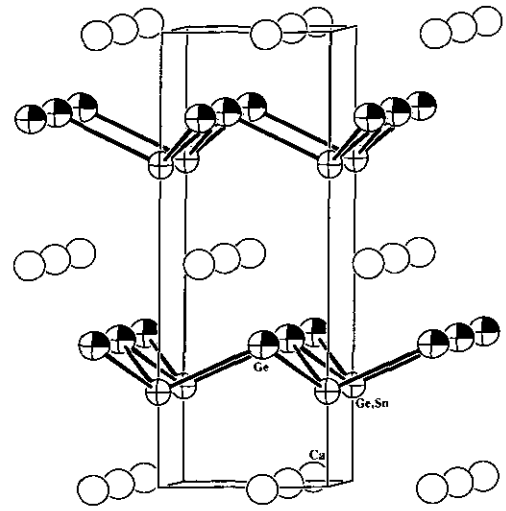

FIG. 3. A side view of the layered structure of $CaSn_{0.5}Ge_{1.5}$ (KSnAs-type). Ca, Ge2,Sn, and Ge1 are shown as open, crossed, and shaded ellipsoids, respectively (94%).

TABLE V

LATTICE AND THERMAL PARAMETERS AND REFINED DISTANCES (Å) IN $CaSn_{0.52(2)}Ge_{1.48(2)}$ ($P6_3mc$)

Atom	x	y	z	B_{eq}	Occup.
Ca	$\frac{1}{3}$	$\frac{2}{3}$	0	1.3(1)	1
Ge1	$\frac{1}{3}$	$\frac{2}{3}$	0.6800(4)	1.20(5)	1
Ge2,Sn	0	0	0.2891(4)	0.86(3)	0.48(2), 0.52(2)
	U_{11}	U_{22}	U_{33}[a]		
Ca	0.016(1)	U_{11}	0.015(2)		
Ge1	0.0161(7)	U_{11}	0.0134(9)		
Ge2,Sn	0.0106(5)	U_{11}	0.0117(6)		
Ca–Ge1 (×3)	3.014(3)		Ge2,Sn–Ge1 (×3)	2.629(1)	
Ca–Ge1	3.296(4)		Ge2–Ca (×3)	3.220(3)	
Ca–Ge2,Sn (×3)	3.220(3)		Ge2–Ca (×3)	3.810(3)	
Ca–Ge2,Sn (×3)	3.810(3)				
			Ge1–Ge2,Sn–Ge1	103.06(6)	
Ge1–Ge2,Sn (×3)	2.629(1)				
Ge1–Ca (×3)	3.014(3)				
Ge1–Ca	3.296(4)				

[a] $U_{12} = U_{22}/2$; $U_{13} = U_{23} = 0$.

equilibrium with CaSn and $CaSn_3$ near 800°C. The Ge1 and Ge2,Sn members each have three short bonds to the other and generate puckered layers of the tetregen elements with calcium in nominal octahedral holes between them, further from the larger tin-substituted position.

This phase is a simple conceptual derivative of the layer $CaSi_2$-type structure (rhombohedral $R\bar{3}m$ (*16*)). The puckered layers in all such examples are isoelectronic and isosteric with rhombohedral As, the layers now being separated by calcium or other cations. $CaSn_{0.5}Ge_{1.5}$ is an hexagonal version with only a two layer sequence, the two positions in each layer again being crystallographically distinct. The long interlayer bonds in CaZnSn ($CaIn_2$) have thus been opened up by a two-electron reduction. This and a better packing also lead to substantial increases in the *c*-axis as well as in the puckering within the layers where a 12° decrease in $\angle B$–X–B is seen. The shorter Ca–$Sn_{0.5}Ge_{0.5}$ separation is now 0.05 Å *greater* than Ca–Sn in CaZnSn. The calcium environment is a trigonal antiprism of the two metalloid types that is capped on one end by a somewhat more distant Ge1.

The expected closed-shell nature of the anion layers [$3b$-Ge(Sn)$^-$ $\hat{=}$ $3b$-P°] and a Zintl phase classification are in accord with the measured diamagnetism, $\chi_M = -0.8 \times 10^{-4}$ emu/mole after core correction (-0.27×10^{-4} emu/mole). There appears to be only one other well established example of this structure type, KSnAs, although the semiconducting KSnSb is basically isostructural with the metalloid sites at least differentiated if not ordered (*14, 19*).

Acknowledgments

The authors thank J. Shinar for the use of the Q-apparatus and J. E. Ostenson and D. K. Finnemore for the magnetic data.

References

1. A. M. GULOY AND J. D. CORBETT, unpublished research.
2. A. K. GANGULI AND J. D. CORBETT, unpublished research.

3. Y.-U. KWON, S. C. SEVOV, AND J. D. CORBETT, *Chem. Mater.* **2,** 550 (1990).
4. A. IANDELLI, *Rev. Chim. Mineral* **24,** 28 (1987).
5. J. SHINAR, B. DEHNER, B. J. BEAUDRY, AND D. T. PETERSON, *Phys. Rev. B* **37,** 2066 (1988).
6. N. WALKER AND D. STUART, *Acta Crystallogr. Sect. A* **39,** 158 (1983).
7. SHELXS-86, G. M. SHELDRICK, Universität Göttingen, BRD (1986).
8. TEXSAN, version 6.0 package, Molecular Structure Corp., The Woodlands, TX (1990).
9. A. IANDELLI, *Z. Anorg. Allg. Chem.* **330,** 221 (1964).
10. M. L. FORNASINI AND F. MERLO, *Acta Crystallogr. Sect. B* **36,** 1739 (1980).
11. M. L. FORNASINI AND F. MERLO, *J. Less-Common Met.* **79,** 111 (1981).
12. F. MERLO, M. PANI AND M. L. FORNASINI, *J. Less-Common Met.* **171,** 329 (1991).
13. P. VILLARS AND L. D. CALVERT, "Pearson's Handbook of Crystallographic Data," Vol. 1, 2nd ed., p. 967. ASM International, Metals Park, OH (1991).
14. J. KLEIN AND B. EISENMANN, *Mat. Res. Bull.* **23,** 587 (1988).
15. H.-U. SCHÜSTER, *Nova Acta Leopoldina* **59,** 199 (1985).
16. B. G. HYDE AND S. ANDERSSON, "Inorganic Crystal Structures," p. 88 Wiley, New York (1989).
17. H. SCHÄFER, *Ann. Rev. Mater. Sci.* **15,** 1 (1985).
18. J. BÖHN AND O. HASSEL, *Z. Anorg. Allg. Chem.* **160,** 152 (1927).
19. K.-H. LII AND R. C. HAUSHALTER, *J. Solid State Chem.* **67,** 374 (1987).